NEUROSCIENCE

Long-duration hippocampal sharp wave ripples improve memory

Antonio Fernández-Ruiz[1]*, Azahara Oliva[1,2]*, Eliezyer Fermino de Oliveira[1,3], Florbela Rocha-Almeida[1,4], David Tingley[1], György Buzsáki[1,5]†

Hippocampal sharp wave ripples (SPW-Rs) have been hypothesized as a mechanism for memory consolidation and action planning. The duration of ripples shows a skewed distribution with a minority of long-duration events. We discovered that long-duration ripples are increased in situations demanding memory in rats. Prolongation of spontaneously occurring ripples by optogenetic stimulation, but not randomly induced ripples, increased memory during maze learning. The neuronal content of randomly induced ripples was similar to short-duration spontaneous ripples and contained little spatial information. The spike content of the optogenetically prolonged ripples was biased by the ongoing, naturally initiated neuronal sequences. Prolonged ripples recruited new neurons that represented either arm of the maze. Long-duration hippocampal SPW-Rs replaying large parts of planned routes are critical for memory.

Sharp wave ripples (SPW-Rs) in the hippocampus are considered a key mechanism for memory consolidation and action planning (*1*–*17*). SPW-Rs are composed of the sharp wave, a negative polarity deflection in the CA1 apical dendritic layer, which reflects the magnitude of the CA3 excitatory input, and the ripple, a short-lived fast oscillatory pattern (140 to 200 Hz) of the local field potential (LFP) in the CA1 pyramidal layer (*1*, *18*–*20*). The duration of ripples exhibited a skewed distribution (Fig. 1, A to C). A minority of long-duration ripples was interspersed among a majority of short- and intermediate-duration events (*9*, *11*). We hypothesized that long-duration ripples are related to mnemonic demand and, therefore, examined ripple statistics across a variety of tasks in rats. The duration of ripples that occurred during immobility periods on a novel maze was longer (Fig. 1B) ($P < 10^{-93}$; rank-sum test; $n = 14$ rats), the fraction of long ripples (>100 ms) was increased ($P < 10^{-3}$; rank-sum test), and the proportion of ripple doublets and triplets increased significantly compared with ripples on a familiar maze in the same animals ($P < 10^{-3}$ and 10^{-2}; rank-sum test) (fig. S1). In addition, the duration of awake ripples in tasks requiring memory (T-maze and M-maze delayed alternation, cheeseboard maze) was longer compared with tasks without a memory-demand requirement (open field exploration, linear or circular track running) (Fig. 1C) ($P < 10^{-90}$), as were both the proportion of long ripples ($P < 10^{-9}$) and the proportion of ripple doublets and triplets (fig. S1) ($P < 10^{-10}$ and 10^{-4}). Correct trials in the M-maze were associated with significantly longer ripples compared with error trials (Fig. 1D) ($P < 10^{-5}$ for correct versus error trials in the same session; sign-rank test), and both ripple duration and proportion of long ripples decreased as learning progressed (fig. S2) ($P < 0.001$ and 0.05, Kruskal-Wallis test). In contrast, the frequency and amplitude of ripples were largely similar across conditions (fig. S1). These observations suggest that the hippocampus generates longer-duration ripple events when memory demands are high.

Next, we examined the neuronal mechanisms underlying the differences between short (≤100 ms) and long-duration (>100 ms) ripples. Confirming the LFP measures, the spiking activity of both putative pyramidal cells and putative interneurons during ripples lasted longer in a novel environment (compared with a familiar one) and in memory tasks (compared with nonmemory tasks) (fig. S1) ($P < 0.01$ and 0.001; rank-sum test; $n = 11$ and 19 rats, respectively). The baseline firing rate of single neurons, calculated from the entire sleep-wake session, was positively correlated with the neuron's participation probability in SPW-Rs (Fig. 1E) ($P < 10^{-100}$ and 10^{-83}; Pearson's correlation; for $n = 3080$ CA1 pyramidal cells and $n = 508$ interneurons in 19 rats). The average rank order of a neuron's within-ripple sequence negatively correlated with that neuron's baseline firing rate (Fig. 1F) ($P < 10^{-82}$ and 10^{-53}) and its participation probability in SPW-Rs (Fig. 1G) ($P < 10^{-53}$ and 10^{-52}). Longer-duration ripples were characterized by the recruitment of more CA1 neurons with lower baseline firing rates (Fig. 1H) ($P < 10^{-35}$ and 10^{-21}).

To test the hypothesis that longer ripples are beneficial for memory, we optogenetically prolonged them. We virally expressed channelrhodopsin 2 (ChR2) in dorsal CA1 pyramidal cells bilaterally (Fig. 2A and fig. S3). At 3 weeks after virus injection, we implanted recording electrodes in area CA1 and placed optic fibers above the pyramidal layer (three per hemisphere along the septotemporal axis) (Fig. 2B). Before behavioral testing, the magnitude of optogenetic stimulation was adjusted to induce ripple-like oscillations with similar frequency and duration to spontaneously occurring ripples (Fig. 2C and fig. S4) (*18*, *21*). To prolong spontaneous ripples, online detection of ripples (fig. S5) triggered a tapered-onset 100-ms-long light stimulus (Fig. 2C), which approximately doubled the duration of each ripple and associated neuronal firing (Fig. 2, D and E, and fig. S4) ($P < 10^{-86}$ for ripple duration and $P < 10^{-19}$ for pyramidal cell firing in spontaneous and prolonged ripples; rank-sum test). In control sessions, optogenetic stimulation followed the ripple by a random delay (400 to 1000 ms) (Fig. 2C).

We tested the consequence of closed-loop ripple prolongation on memory performance in a hippocampus-dependent M-maze task (Fig. 3A) (*22*). Rats were rewarded on the M-maze each time they visited the end of one of the three maze arms in the correct task sequence (center-left-center-right-center, and so on) (Fig. 3A). This task has two parts: In the "outbound" alternation part, the rat starts in the central arm and, after a 20-s delay, must chose the side arm opposite the most recently visited one to receive a sugar-water reward (*7*). In the "inbound" part, the rat has to return to the center arm from either of the side arms without a delay. The outbound component of the task has been shown to be impaired with SPW-R disruption but not the inbound part (*7*). The effect of closed-loop elongation of ripples on memory performance was compared to two control conditions: sessions in which optogenetic stimulation was delivered at randomly delayed intervals (Fig. 2C) after the detected ripple ("random" condition) and sessions with a "no-stimulation" control condition. Two sessions (30 min each) were conducted on each of 10 days (a.m. and p.m.), comparing two conditions in a given cohort (ripple prolongation versus no stimulation or random stimulation, and random stimulation versus no stimulation; five rats in each of three cohorts, plus another "sham" cohort of five rats with no stimulation) (fig. S7C). The majority of both short and long ripples occurred in the delay period, followed by the reward-side areas (Fig. 3B and fig. S6). Because performance of the no-stimulation and sham groups did not differ (fig. S6C) [$P > 0.05$; repeated measures analysis of variance (ANOVA); main effect of group], subjects were combined into a single no-stimulation control group. Closed-loop ripple prolongation significantly increased performance on the outbound component of the task when compared with no-stimulation or random-stimulation controls (Fig. 3C) (main effect of group; $P < 10^{-10}$; repeated measures ANOVA), whereas no difference was found between the no-stimulation and random-stimulation sessions ($P > 0.05$) (fig. S7C). These differences were present both when comparing all animals per condition across days (Fig. 3C) and different conditions in the same animal and day (figs. S7 and S8). The number of days to reach the 80% correct choice criterion was

[1]New York University Neuroscience Institute, New York University, New York, NY 10016, USA. [2]Department of Neuroscience and Zuckerman Mind Brain Behavior Institute, Columbia University, New York, NY 10027, USA. [3]Center for Mathematics, Computing and Cognition, Universidade Federal do ABC, São Bernardo do Campo, São Paulo, Brazil. [4]Division of Neurosciences, University Pablo de Olavide, 41013 Seville, Spain. [5]Center for Neural Science, New York University, New York, NY 10016, USA.
*These authors contributed equally to this work.
†Corresponding author. Email: gyorgy.buzsaki@nyumc.org

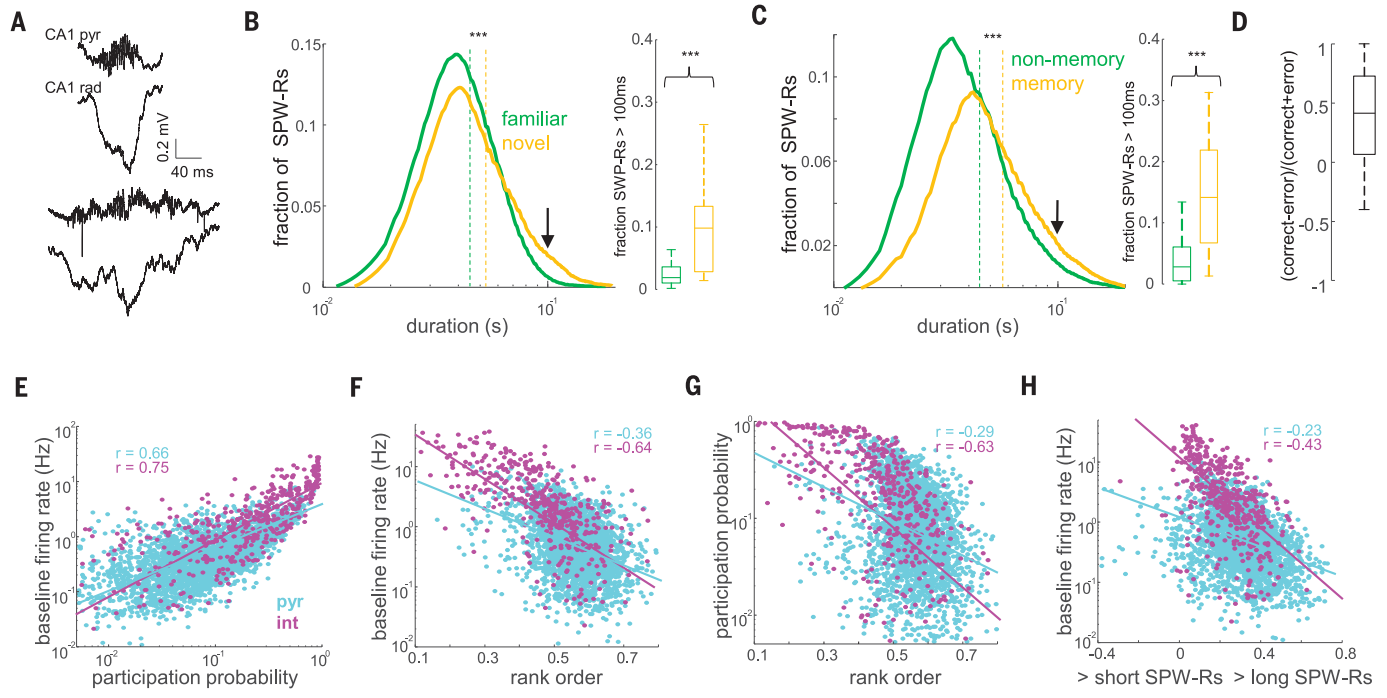

Fig. 1. Longer-duration waking SPW-Rs occur more frequently under increased memory demand. (**A**) Examples of short (top) and long (bottom) SPW-Rs during waking state. pyr, pyramidal; rad, stratum radiatum. (**B**) Distribution of the durations of SPW-Rs in familiar and novel environments (n = 16,732 and 7495 SPW-Rs, respectively, from 14 rats). Dashed lines indicate medians. The fraction of long SPW-Rs (>100 ms, indicated with an arrow) is shown in the right panel. ***P < 0.001; rank-sum test. (**C**) Distribution of the durations of SPW-Rs and the fraction of long SPW-Rs in memory-demanding and nonmemory tasks (see supplementary materials and methods) (n = 33,690 and 31,637 SPW-Rs, respectively, from 31 rats). (**D**) Proportion of SPW-Rs >100 ms in the delay box of the M-maze prior to correct versus error trials (ratio per session; n = 45 sessions from 10 rats). (**E**) Correlation between the baseline firing rate and mean participation probability in SPW-Rs for CA1 pyramidal cells ($P < 10^{-100}$) and interneurons (int) ($P < 10^{-83}$). (**F**) Correlation between the baseline firing rate and the mean rank order in SPW-Rs (pyr, $P < 10^{-82}$; int, $P < 10^{-53}$). (**G**) Correlation between the mean participation probability and the mean rank order in SPW-Rs (pyr, $P < 10^{-52}$; int, $P < 10^{-52}$). (**H**) Firing rate as a function of that neuron's probability of firing in long versus short SPW-Rs [(long − short)/(long + short)] (pyr, $P < 10^{-35}$; int, $P < 10^{-29}$).

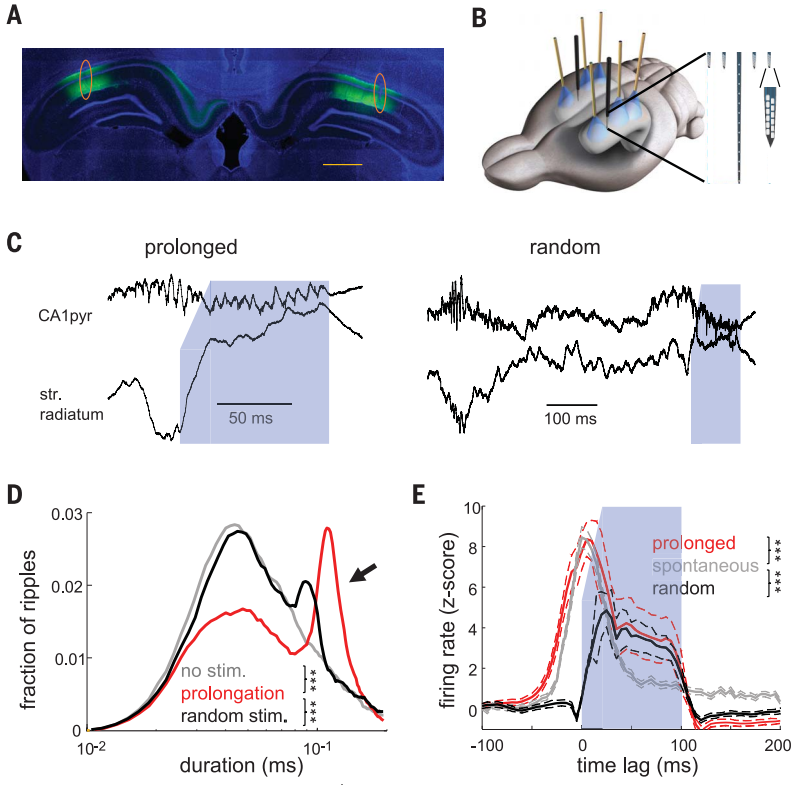

Fig. 2. Closed-loop optogenetic prolongation of ripples. (**A**) CamKII-ChR2-EYFP expression (green) in the dorsal hippocampus. Blue is 4′,6-diamidino-2-phenylindole (DAPI) staining. Orange circles show electrode tracks. Scale bar, 1 mm. (**B**) Three optic fibers and silicon probe arrays were implanted above the dorsal-posterior CA1 pyramidal layer. (Inset) Detail of silicon probe tips. (**C**) Examples of closed loop–prolonged ripple (left) and induced ripple at a random delay after the SPW-R (right). Blue shading indicates duration of light activation (100 ms). Sharp wave is absent in stratum radiatum (str. radiatum) during optogenetic stimulation. (**D**) Distribution of ripple durations in no-stimulation, ripple-prolongation, and random-stimulation sessions (n = 10 sessions of each type from 10 rats). (**E**) Z-scored firing ± SEM rates of pyramidal neurons during spontaneous and induced ripples (n = 1116 units for prolonged and spontaneous ripples and n = 705 for random stimulation from 5 rats). Onset of stimulation or peak of ripple power at 0 ms. ***P < 0.001; rank-sum test.

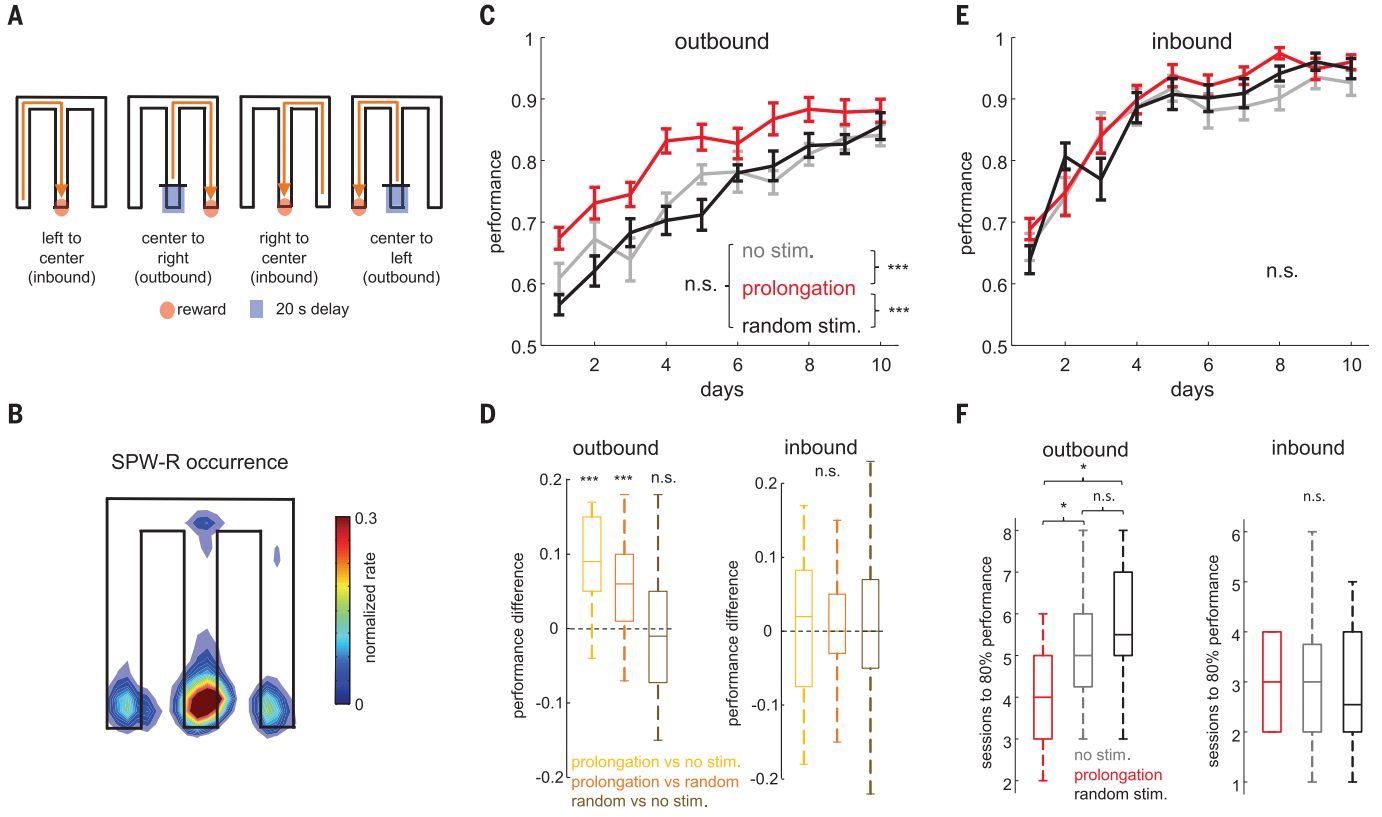

Fig. 3. Ripple prolongation improves memory. (**A**) Schematic of the M-maze task. Red dot, reward area; blue square, start area (20-s delay). (**B**) Distribution of SPW-R occurrence in the M-maze (n = 33,179 SPW-Rs from 10 rats). (**C** and **D**) Fraction of correct trials (mean ± SEM) in the M-maze task during outbound (C) and inbound (D) runs in no-stimulation, ripple-prolongation, and random-stimulation sessions (total of 20 rats). ***P < 0.001; Tukey's post-hoc test. n.s., not significant. (**E**) Performance ratios for the same day and animal for ripple-prolongation versus no-stimulation sessions, ripple-prolongation versus random-stimulation sessions, or random-stimulation versus no-stimulation sessions in all animals (n = 20). ***P < 0.001; two-sided Wilcoxon signed-rank test. (**F**) Session number in which animals reached performance criterion of 80% correct trials. *P < 0.05; rank-sum test.

reached significantly earlier in the closed-loop condition when compared with either the no-stimulation or random-stimulation conditions (Fig. 3F) (P < 0.05; rank-sum test). Ripple prolongation had no impact on the inbound component of the task (Fig. 3, D to F) (main effect of group; P > 0.05; repeated-measures ANOVA). The number of ripples per session, the number of trials in the 30-min sessions, mean running speed, theta frequency, and theta/delta band ratio did not significantly differ across the different groups (fig. S6).

In five of the AAV-CaMKII-ChR2–injected rats, we tested how truncation of SPW-Rs affected performance after a 1-week rest period. Short-duration (10 ms), high-intensity pulses were used to abort ripples. Preventing the occurrence of long-duration ripples resulted in significant deterioration of performance in the outbound, but not inbound, trials compared with random-stimulation controls (fig. S9), similar to results obtained with electrical disruption of ripples (*7*).

Searching for a physiological mechanism of the memory-improving effect of elongated ripples, we compared properties of neurons during spontaneous SPW-Rs with those recruited by optogenetic stimulation. The participating neurons active in spontaneous and optogenetically prolonged ripples were similar, as demonstrated by the significant correlations of the ripple-participation index (i.e., the probability to fire within ripples) [spontaneous versus random, $P < 10^{-38}$ and 10^{-36} for pyramidal cells and interneurons (Fig. 4A); spontaneous versus prolonged, $P < 10^{-25}$ and 10^{-7} (Fig. 4B)] and firing rates between conditions (fig. S11) (*18*). Within an elongated ripple, a given pyramidal cell typically fired either in the early (spontaneous) or the optogenetically prolonged (late) part of the ripple (Fig. 4C) (0.51 ± 0.01 and 0.43 ± 0.01 fractions) but rarely in both parts (0.06 ± 0.03%; $P < 10^{-100}$; sign-rank test). The diversity of neurons (fraction of different cells participating) in prolonged ripples was thus significantly higher compared with randomly induced ripples and spontaneous short ones (Fig. 4D) ($P < 10^{-60}$ and 10^{-100}; rank-sum test). Fast firing neurons tended to fire in the early part of the prolonged ripples, whereas neurons added to the ongoing sequence in the prolonged part were recruited mainly from the lower firing rate population (Fig. 4, E and F) ($P < 10^{-6}$ and 10^{-6} for pyramidal cells and interneurons, respectively). In addition, in prolonged ripples, a larger proportion of neurons had place fields on the maze compared with spontaneous or random ripples (P < 0.01 and 0.001; rank-sum test). Pyramidal cells recruited in prolonged and spontaneously long SPW-Rs also contained more spatial information and were more spatially selective and less sparse than those in short SPW-Rs and randomly induced ripples (fig. S12). Closed loop–prolonged ripples are thus not simply the summation of spontaneous and randomly induced events but reflect a recruitment of a different population of neurons with relevant spatial information, reminiscent of the more diverse neuronal population of long-duration spontaneous ripple events (Fig. 4D) (short versus long spontaneous ripples; $P < 10^{-100}$) (figs. S10 to S12).

We examined the relationship between spike content of ripples and place-related firing in the maze. First, we considered place cells that had the highest participation probability (first quartile) in either the early or late parts of the different types of ripples (spontaneous short, spontaneous long, prolonged, and random) and plotted the distribution of their place fields on the maze. Neurons that preferred to fire in the late part of spontaneously long or prolonged ripples had more place fields on the side arms of the maze and fewer in the center arm during

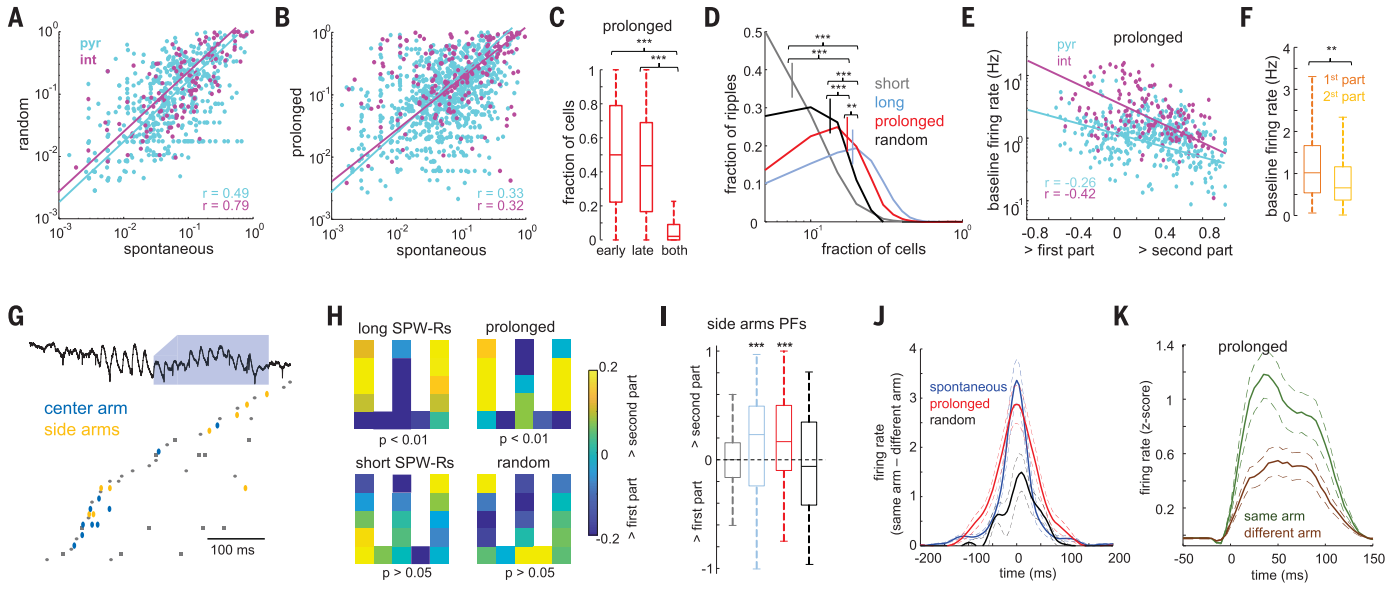

Fig. 4. Spontaneously long and optogenetically prolonged ripples contain more-diverse task-related activity. (**A** and **B**) Correlation of neuron participation probability between spontaneous and random delay–induced ripples (A) and between spontaneous and prolonged ripples (B). (**C**) Probability of firing in the early-only, late-only, or both parts of prolonged ripples. ***P < 0.001; sign-rank test. (**D**) Distribution of the fraction of all recorded neurons participating in each ripple type. Short and long (>100 ms) spontaneous SPW-Rs were analyzed separately. **P < 0.01; ***P < 0.001; rank-sum test. (**E**) Firing rate as a function of that neuron's probability of firing in the spontaneous versus closed loop–prolonged part of the ripple ($P < 10^{-7}$). Only cells with participation probability of at least 0.05 were included. (**F**) Baseline firing rate of neurons with maximum participation in the spontaneous and closed loop–prolonged parts of the ripple. **P < 0.001; rank-sum test. (**G**) Example replay sequence of travel trajectory during a prolonged ripple. Neurons representing the central and side arms fire mainly during the spontaneous and prolonged parts of the ripple, respectively. Ellipsoids indicate pyramidal cells; squares indicate interneurons. (**H**) Distribution of place fields of neurons with higher participation probability in either the early or late part of different types of ripples. P values correspond to Fisher's exact test. (**I**) Proportion of place cells with side arm–specific fields that fired with higher probability in either the first or the second part of ripples. ***P > 0.001; rank-sum test. (**J**) Differences of spike cross-correlations between z-scored firing rates of neurons representing the same or different side arms during ripples (P < 0.05 between spontaneous and prolonged ripples versus random ones; rank-sum test). (**K**) Cross-correlations between neurons' z-scored firing rates in the spontaneous and induced parts of prolonged ripples, shown separately for neurons representing the same or different side arms (P < 0.05; signed-rank test).

outbound travels compared with cells that fired in the early part (Fig. 4H). Second, we identified neurons with side arm–unique place fields during outbound travels and calculated their spike occurrence in the first and second halves of spontaneous and induced ripples. Side arm–unique place cells fired at higher probability during the second part of closed loop–prolonged and spontaneous long ripples (Fig. 4I) (P < 0.01 and 0.001; sign-rank test) but not during spontaneous short or random-delay optogenetically induced ripples (P > 0.05). There was an inverse correlation between place cells active in the left or right side arm in different ripples. During both spontaneous and prolonged ripples, the likelihood of neurons encoding the same side arms firing together was higher than that of neurons encoding opposite arms (Fig. 4J) ($P < 10^{-4}$ and 10^{-5}; rank-sum test). The difference between these likelihoods was significantly lower for random ripples (P < 0.05 and 0.05 for spontaneous and prolonged against random ripples; rank-sum test). When we compared spikes occurring in the spontaneous and optogenetically prolonged parts of closed loop–induced ripples, the cross-correlation was significantly stronger for neurons representing the same side arms than those representing opposite side arms (Fig. 4K) (P < 0.05; sign-rank test) and was similar to spontaneous SPW-Rs (fig. S12).

Our findings demonstrate that a simple measure, such as the duration of SPW-Rs, can provide valuable information about the underlying neuronal computations. Learning and correct recall in spatial memory tasks were associated with extended SPW-Rs (Fig. 1). Closed-loop optogenetic prolongation of CA1 ripples improved working memory performance (Fig. 3), whereas aborting the late part of ripples decreased performance (*7*). Prolongation of CA1 ripples did not induce repeated spiking of the already active neurons but instead recruited spikes from the low-firing population of pyramidal cells and increased the diversity of the participating neurons. Neurons recruited during the artificially elongated portion of ripples had place fields preferentially in the side arms of the maze (Fig. 4). This feature of the optogenetically prolonged ripples resembled those in spontaneous long ripple events. In contrast, randomly induced ripples recruited largely the same neurons as in short spontaneous ripples (*18*) (Fig. 4). We hypothesize that the neuronal trajectory of optogenetically induced events depends on the contemporaneous brain state (Fig. 4, D and E) (*13*, *23*, *24*), with SPW-Rs and inter-SPW-R periods referring to different network states. Once a trajectory has been selected at the onset of a SPW-R, artificial recruitment of additional neurons via optogenetic perturbation is constrained by the attractor dynamic of the CA1 network (*11*, *25*). This observation supports the idea that CA1 neuronal sequences are computed locally in CA1 (*18*, *26*) rather than being fully inherited from upstream regions (*1*, *11*, *27*). Alternatively, SPW-Rs are embedded in larger networks, including entorhinal and neocortical areas (*21*, *28*–*30*), and the differential effects of closed-loop and random stimulation might be determined by the network state in areas upstream from CA1. In either case, diversification of neurons, covering large segments of planned routes, may explain the memory-improving effect of both spontaneous long and closed loop–prolonged ripples.

REFERENCES AND NOTES

1. G. Buzsáki, *Hippocampus* **25**, 1073–1188 (2015).
2. K. Diba, G. Buzsáki, *Nat. Neurosci.* **10**, 1241–1242 (2007).

3. D. J. Foster, M. A. Wilson, *Nature* **440**, 680–683 (2006).
4. H. Xu, P. Baracskay, J. O'Neill, J. Csicsvari, *Neuron* **101**, 119–132.e4 (2019).
5. A. S. Gupta, M. A. A. van der Meer, D. S. Touretzky, A. D. Redish, *Neuron* **65**, 695–705 (2010).
6. S. Takahashi, *eLife* **4**, e08105 (2015).
7. S. P. Jadhav, C. Kemere, P. W. German, L. M. Frank, *Science* **336**, 1454–1458 (2012).
8. D. Dupret, J. O'Neill, B. Pleydell-Bouverie, J. Csicsvari, *Nat. Neurosci.* **13**, 995–1002 (2010).
9. T. J. Davidson, F. Kloosterman, M. A. Wilson, *Neuron* **63**, 497–507 (2009).
10. C. Drieu, R. Todorova, M. Zugaro, *Science* **362**, 675–679 (2018).
11. B. E. Pfeiffer, D. J. Foster, *Science* **349**, 180–183 (2015).
12. M. P. Karlsson, L. M. Frank, *Nat. Neurosci.* **12**, 913–918 (2009).
13. G. Dragoi, S. Tonegawa, *Nature* **469**, 397–401 (2011).
14. H. F. Ólafsdóttir, D. Bush, C. Barry, *Curr. Biol.* **28**, R37–R50 (2018).
15. M. A. Wilson, B. L. McNaughton, *Science* **265**, 676–679 (1994).
16. G. Girardeau, K. Benchenane, S. I. Wiener, G. Buzsáki, M. B. Zugaro, *Nat. Neurosci.* **12**, 1222–1223 (2009).
17. T. Nakashiba, D. L. Buhl, T. J. McHugh, S. Tonegawa, *Neuron* **62**, 781–787 (2009).
18. E. Stark, L. Roux, R. Eichler, G. Buzsáki, *Proc. Natl. Acad. Sci. U.S.A.* **112**, 10521–10526 (2015).
19. J. O'Keefe, L. Nadel, *The Hippocampus as a Cognitive Map* (Oxford Univ. Press, 1978).
20. A. Oliva, A. Fernández-Ruiz, G. Buzsáki, A. Berényi, *Neuron* **91**, 1342–1355 (2016).
21. A. Oliva, A. Fernández-Ruiz, E. Fermino de Oliveira, G. Buzsáki, *Cell Rep.* **25**, 1693–1700.e4 (2018).
22. S. M. Kim, L. M. Frank, *PLOS ONE* **4**, e5494 (2009).
23. E. Pastalkova, V. Itskov, A. Amarasingham, G. Buzsáki, *Science* **321**, 1322–1327 (2008).
24. M. Tsodyks, T. Kenet, A. Grinvald, A. Arieli, *Science* **286**, 1943–1946 (1999).
25. N. Maingret, G. Girardeau, R. Todorova, M. Goutierre, M. Zugaro, *Nat. Neurosci.* **19**, 959–964 (2016).
26. R. M. Memmesheimer, *Proc. Natl. Acad. Sci. U.S.A.* **107**, 11092–11097 (2010).
27. M. F. Carr, M. P. Karlsson, L. M. Frank, *Neuron* **75**, 700–713 (2012).
28. J. Yamamoto, S. Tonegawa, *Neuron* **96**, 217–227.e4 (2017).
29. J. O'Neill, C. N. Boccara, F. Stella, P. Schoenenberger, J. Csicsvari, *Science* **355**, 184–188 (2017).
30. S. P. Jadhav, G. Rothschild, D. K. Roumis, L. M. Frank, *Neuron* **90**, 113–127 (2016).

ACKNOWLEDGMENTS

We thank J. Makara, S. Mckenzie, G. Kozak, P. Petersen, L. Sjulson, R. Swanson, V. Varga, and M. Valero for insightful comments and M. Soula for technical assistance. **Funding:** This work was supported by a Sir Henry Wellcome Postdoctoral Fellowship (A.F.-R.), EMBO Postdoctoral Fellowship ALTF 120-2017 (A.O.), FAPESP grant 2017/03729-2 (E.F.d.O.), NIH (MH107396 and NS074015 to G.B. and U19NS104590), and NSF 1707316 (NeuroNex MINT). **Author contributions:** A.F.-R. and G.B. conceived of and designed the experiments; A.F.-R. and E.F.d.O. performed experiments; F.R.-A. performed immunohistological experiments; A.F.-R. and A.O. analyzed data; and G.B., A.F.-R., A.O., and D.T. wrote the manuscript. **Competing interests:** The authors declare that they have no competing interests. **Data and materials availability:** All data needed to evaluate the conclusions in the paper are present in the paper and/or the supplementary materials. Part of the dataset included in this study is already available in the CRCNS.org and in the buzsakilab.com databases. The remaining data will be deposited in the same databases and are immediately available upon reasonable request. Custom Matlab scripts can be downloaded from https://github.com/buzsakilab/buzcode.

SUPPLEMENTARY MATERIALS

science.sciencemag.org/content/364/6445/1082/suppl/DC1
Materials and Methods
Figs. S1 to S12
Table S1
References (*31–40*)

19 February 2019; accepted 1 May 2019
10.1126/science.aax0758

Science

Long-duration hippocampal sharp wave ripples improve memory

Antonio Fernández-Ruiz, Azahara Oliva, Eliezyer Fermino de Oliveira, Florbela Rocha-Almeida, David Tingley and György Buzsáki

Science **364** (6445), 1082-1086.
DOI: 10.1126/science.aax0758

Longer ripples make better memories

Sharp wave ripples in the hippocampus are thought to play a role in memory formation and action planning. Fernández-Ruiz *et al.* used multisite electrophysiological recordings combined with optogenetic activation of hippocampal pyramidal neurons in rats performing learning tasks. Learning and correct recall in spatial memory tasks were associated with extended sharp wave ripples. Artificially prolonging these ripples improved working memory performance, whereas aborting the late part of ripples decreased performance.

Science, this issue p. 1082